computation

Article

A New Modeling Approach for Viscous Dampers Using an Extended Kelvin–Voigt Rheological Model Based on the Identification of the Constitutive Law's Parameters

Ovidiu Vasile and Mihai Bugaru *

Department of Mechanics, University POLITEHNICA of Bucharest, 060042 Bucharest, Romania
* Correspondence: skmbugaru@yahoo.com; Tel.: +40-739966136

Abstract: In addition to elastomeric devices, viscous fluid dampers can reduce the vibration transmitted to dynamic systems. Usually, these fluid dampers are rate-independent and used in conjunction with elastomeric isolators to insulate the base of buildings (buildings, bridges, etc.) to reduce the shocks caused by earthquakes by increasing the damping capability. According to the EN 15129 standard, the velocity-dependent anti-seismic devices are Fluid Viscous Dampers (FVDs) and Fluid Spring Dampers (FSDs). Based on experimental data from a dynamic regime of a fluid viscous damper of small dimensions, for which not all the design details are known, to determine the law of behavior for the viscous damper, the characteristics of the damper are identified, including the nonlinear parameter α (exponent of velocity V) of the constitutive law. Note that the magnitude of the fluid damper force depends on both velocity (where the maximum value is 0.52 m/s) and amplitude displacement ($\pm$25 mm). Using the Kelvin–Voigt rheological models, the dynamic response of a structure fixed with a fluid viscous device is analyzed, presenting the reaction force and displacement during the parameterized application of an external shock. This new approach for FVDs/FSDs was validated using the standard deviation between the experimental data and the numerical results of the extended Kelvin–Voigt model offering researchers in the field of seismic devices a reliable method to obtain a constitutive law for such devices.

Keywords: extended Kelvin–Voigt rheological model; viscous dampers; nonlinear viscous damping; energy dissipation

Citation: Vasile, O.; Bugaru, M. A New Modeling Approach for Viscous Dampers Using an Extended Kelvin–Voigt Rheological Model Based on the Identification of the Constitutive Law's Parameters. *Computation* **2023**, *11*, 3. https://doi.org/10.3390/computation11010003

Academic Editor: Demos T. Tsahalis

Received: 28 November 2022
Revised: 16 December 2022
Accepted: 21 December 2022
Published: 27 December 2022

1. Introduction

The viscous damper is recommended to operate at the energy levels specified by the structural engineer without degradation of performance or service reduction [1]. Sadek and Riley investigated in [2] the effect of increased viscous damping on the seismic response of structures. A viscous fluid damper dissipates energy by forcing a fluid through an orifice, causing a damping pressure and force. In the case of linear viscous dampers, this force is proportional to the relative velocity between the ends of the damper. Verma [3] studied the optimal utilization of viscous dampers, modeled using Maxwell's model of viscoelasticity, for seismic performance improvements in structures. Berkovsky et al. [4] investigated the modeling of high-viscous dampers for piping protection from earthquakes or other shock loads in nuclear systems. For high-velocity applications, non-linear viscous dampers are used in order to not exceed the force capacity of the device. Whittle et al. [5] created an optimization scenario for buildings using viscous dampers. In [6], Seleemah and Constantinou analyzed, in the first systematic experimental study, the nonlinear viscous damping devices using earthquake simulation tests on one-story and three-story structures for buildings.

The dynamic response of a multi-story steel moment-resisting frame equipped with fluid viscous dampers and subjected to seismic loads was investigated numerically by Martinez-Rodrigo et al. [7]. The main objective of this numerical research was to build a simple methodology leading to an optimum retrofitting option with nonlinear fluid viscous dampers. In these nonlinear devices, the force is a fractional power law of the velocity, and high rates do not lead to forces as high as in the linear case. The parameter identification for basic and generalized Kelvin–Voigt and Maxwell models for fluid viscous dampers and for measuring the difference between analytical and experimental tests were made by Greco et al. [8]. For this purpose, particle swarm optimization was adopted.

The development of the fractional Maxwell model and fractional Kelvin model with experimental data was completed by Xu et al. [9]. In another study, Park [10] found that the standard mechanical model comprising linear springs and dashpots was shown to accurately describe the broad-band rheological behavior of standard viscoelastic dampers and to be more efficient than other models such as the fractional derivative model and the modified power law. Some methods for identification of the parameters of both the Kelvin–Voigt fractional model and the Maxwell fractional model were presented by Lewandowski et al. [11].

Castellano et al. [12] experimentally investigated fluid viscous dampers (FVDs) using the new standard [1]. Mousavi and Ghorbani -Tanha studied [13] the optimum placement and characteristics of linear velocity-dependent dampers in the frequency domain. Pettinga et al. investigated the use of supplemental damping to control structural deformations and forces caused by seismic motions [14]. Using the structural steel frames with energy dissipation provided by FVDs, the LDD was obtained (Law Damage Design) [14].

Cavaleri et al. [15] conducted experimental research concerning the damper constants in the range of law velocities developing the limit of validity of the models for viscous dampers.

In [16], Del Gobbo studied the distribution of dampers within a building and the supplemental damping to obtain the optimal amount of damping and reduce the total building seismic damage. Lamprea-Pineda and Garzon-Amortegui investigated the use and implementation of the nonlinear viscous fluid damper (VFD) in a building [17].

Wong [18] demonstrated the effectiveness of a simple numerical algorithm to predict the time history response of inelastic structures with nonlinear FVDs. The time history and energy responses of inelastic one-story and multi-story frames were evaluated, and the contributions of VFDs with different power-law coefficients and damping coefficients were analyzed and compared.

Altieri et al. [19] investigated the rigorous approach to designing optimal nonlinear viscous dampers based on performance criteria. Comparisons between the series and parallel connections of the hysteretic system and viscous dampers using response spectra analyses of a single degree of freedom structures were completed by Bougteb [20]. For the series model, a semi-implicit solution scheme for the classical Maxwell model was modified to include the inelasticity of the time-independent hysteretic spring.

A modified version of the direct displacement-based design was proposed for the creation of structures equipped with FVDs so that the effect of higher modes and the difference between spectral velocity and pseudo-spectral velocity are applied in the design process, which was studied by Noruzvand et al. [21].

De Domenico et al. [22] studied a practical multi-level performance-based optimization method of nonlinear viscous dampers for seismic retrofit of existing substandard steel frames. In this case, a Maxwell model was adopted to simulate the behavior of the combined damper-supporting brace system with a fractional power-law force–velocity relationship for the nonlinear viscous dampers. The efficiency of the final optimum design solution was also investigated by using drift-based, velocity-based, and energy-based uniform damage distribution approaches to identify the most efficient performance index parameter for optimization purposes.

Michailides [23] developed a numerical analysis method for wave–structure interaction effects using the velocity-dependent viscous damping (VD-PQ) model. Kookalani and Shen [24] investigated the impact of various FVD parameters on structures during an earthquake.

The fundamental problem treated in this study is the identification of the parameters of the constitutive law for a viscous fluid damper using tests performed according to EN 15129 [1]. Starting from the classical model Kelvin–Voigt, a robust method for identifying the nonlinear parameters of the constitutive law using the generalized forms of the model in the frequency domain is developed. Experimental data are obtained from a viscous damper implemented in the generalized Kelvin–Voigt model to identify the constitutive law parameters.

Energy dissipation devices, also called dampers, are classified into two main categories: rate-dependent and rate-independent dampers [25]. In the former, also denominated (linear or nonlinear) viscous dampers, the force depends, fully or partially, on the velocity [26,27]. In the latter, also called hysteretic dampers, the force is only a function of the displacement [28,29].

2. An Extended Rheological Model for Nonlinear Viscous Damper

As stated in European Standard EN 15129 [1], the viscous dampers can be modeled using rate-dependent Kelvin–Voigt rheological hysteresis models. These models are illustrated in Figure 1. Starting from the classical representation of a spring and a damper in parallel, as it can be seen in Figure 1a for the Kelvin–Voigt classical model, it is known that the resistance force of a viscous damper depends on the velocity of deformation of the damper and the amplitude of the deformation.

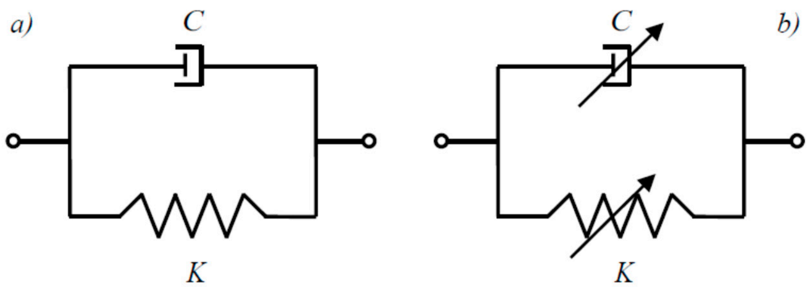

Figure 1. Rheological model: (**a**) Kelvin–Voigt; (**b**) extended Kelvin–Voigt.

The expression for the evaluation of the force exhibited by the damper can be written as follows [7]:

$$F_{KV} = Kx + C\dot{x}, \tag{1}$$

where:

- F_{KV} is the damping (axial) force of the rheological classical Kelvin–Voight model;
- x is the viscous damper displacement;
- $\dot{x}$ is the viscous damper velocity;
- K is the stiffness of the spring element;
- C is the damping coefficient of the viscous element.

Nonlinearity is introduced using the fractional exponents, chosen to generalize the Kelvin–Voigt approach, β and α, which are fractional exponents for both the spring and viscous damper, respectively. In this way, the behavior of the nonlinear viscous damper approach using the extended Kelvin–Voigt model, illustrated in Figure 1b, is described by the equation:

$$F_{KV,g} = Kx^{\beta} + C\dot{x}^{\alpha}, \tag{2}$$

where $F_{KV,g}$ is the axial force of the extended rheological Kelvin–Voigt model.

Therefore, for the classical Kelvin–Voigt model, the characteristic parameters of the viscous damper behavior are K and C, while for the extended Kelvin–Voigt model, the parameters of the nonlinear viscous damper behavior are K, C, β, and α.

3. Experimental Data

The experimental tests were performed in the ICECON Test Laboratory, within ICECON S.A. from Bucharest. Due to the conditions of confidentiality, the authors will not give constructive details of the product or other information from the tests because they are not the subject of this study.

The maximum working velocity of the viscous damper given by the manufacturer is 0.52 m/s. Considering the maximum displacement amplitude of ±25 mm, it is possible to compute the frequency values necessary for the harmonic control signals. The frequency values for the harmonic control signal are given in Table 1.

Table 1. The frequency values vs. maximum rated velocity.

Maximum Rated Velocity [%]	Velocity [m/s]	Frequency [Hz]
1	0.0052	0.033
25	0.13	0.828
50	0.26	1.655
75	0.39	2.483
100	0.52	3.310

In this case, it is considered that the maximum displacement amplitude of ±25 mm allowed using the viscous damper (FVD or FSD) is the same as the seismic design displacement, which means that $d_{bd} = \pm 25$ mm [1]. The damper's restoring force, F_n, at a velocity, v_n, is defined as the average of the intercepts of the second hysteretic loop cycle with an axis parallel to the force axis at 50% of $+d_{bd}$ and $-d_{bd}$ [1], given by the equation:

$$F_n = \frac{F_n^{(+)} + \left|F_n^{(-)}\right|}{2}, \tag{3}$$

where d_{bd} represents the seismic design displacement [1].

The experimental tests were performed in the ICECON Test Laboratory, within ICECON S.A. from Bucharest, in compliance with the requirements of the "Constitutive law test for FVD/FSD" chapter 7 from EN 15129 [1]. Due to the conditions of confidentiality, the authors will not give constructive details of the product or other information from the tests because they are not the subject of this study. The test setup, illustrated in Figure 2, consists of a steel frame with stand loads of tension and compression at 300 kN. The device is anchored to the structure using a pin and connected to the threaded joint's hydraulic actuator rod. The movements are generated using a hydraulic cylinder actuator of 200 kN, controlled in force and/or displacement using a pumping group and a hydraulic servo valve. Between the steel frame and the device is located a load cell of 10 kN which records the forces applied to the device during the experiment. The tests are carried out with the imposition of displacement, and the movement of the device is recorded using a displacement transducer mounted on the device. The control and data acquisition system can generate the displacement of the analysis in real-time through the instantaneous variation of the forces applied with the actuator cylinder using an automatic displacement control system. The time history displacement of ±25 mm is imposed with a harmonic signal generator that respects the velocities and frequencies presented in Table 1.

The experimental data illustrated in Figure 3 are obtained by reading the output FSD reaction. When a harmonic test input is achieved, the maximum imposed velocity is applied only for an instant. It is identified as an FSD according to the requirements of EN 15129 (depending on velocity and amplitude displacement). The FVD output force depends on velocity only and does not change with the damper stroke position. Table 2 presents the normalized force, the normalized velocity, the velocity, and the restoring force.

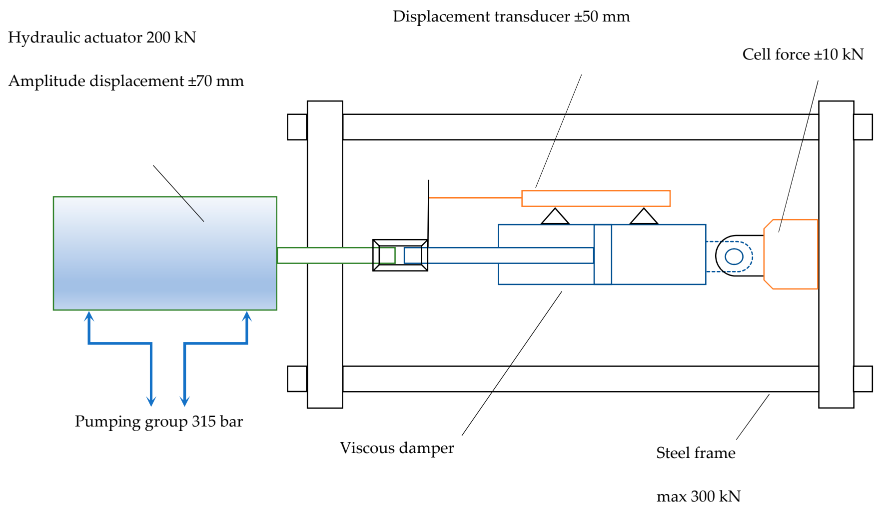

Figure 2. Experimental setup.

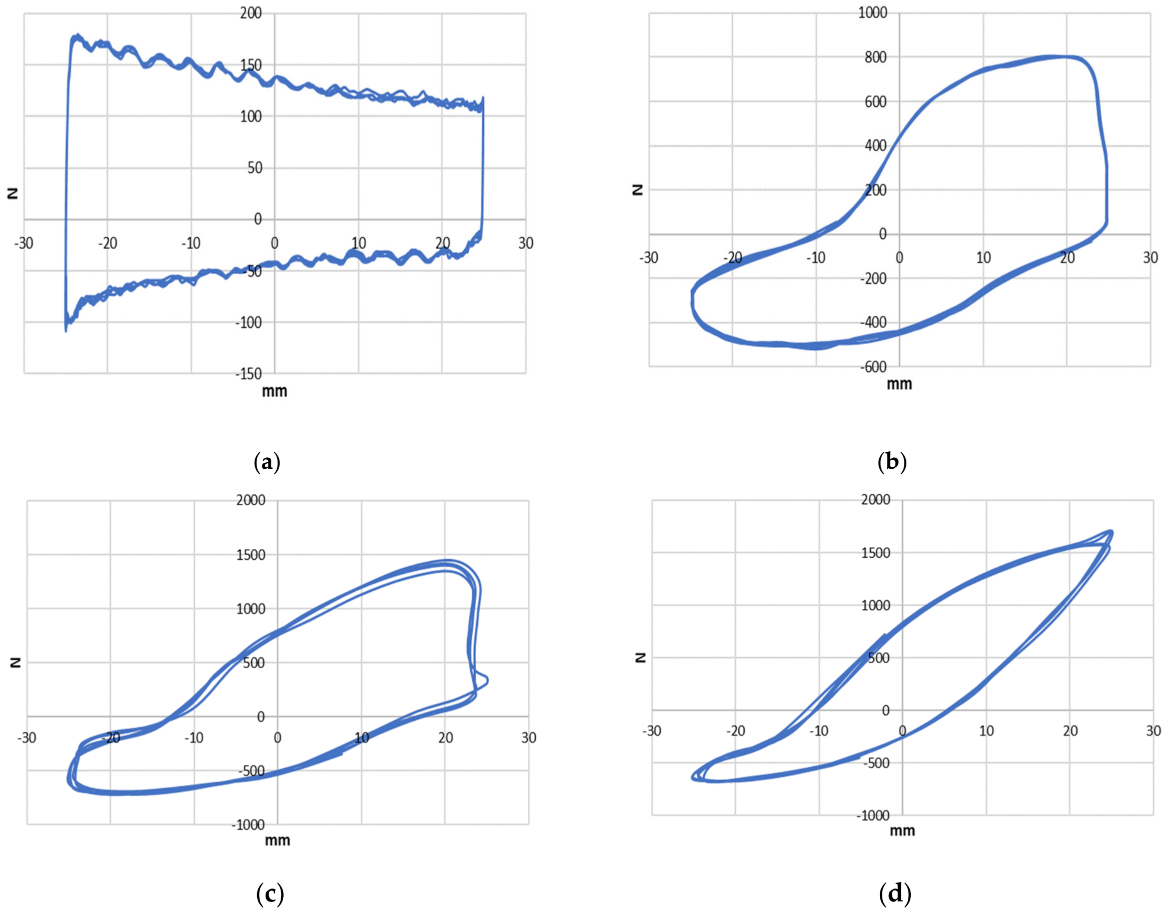

Figure 3. *Cont.*

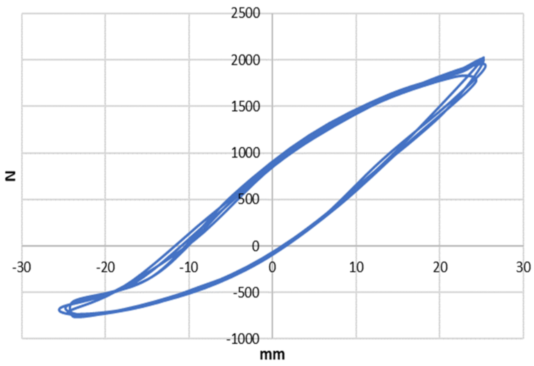

(**e**)

Figure 3. Force-displacement hysteresis loops, with the applied velocity of the maximum rated velocity at (**a**) 1%, (**b**) 25%, (**c**) 50%, (**d**) 75% and (**e**) 100%.

Table 2. The normalized force vs. normalized velocity.

No./ Index	Normalized Velocity [%]	Velocity v [m/s]	Restoring Force F_n [kN]	Normalized Force [%]
1	1	0.0052	0.08889	8.527846
2	25	0.13	0.63013	60.45282
3	50	0.26	0.93926	90.10985
4	75	0.39	0.96099	92.19456
5	100	0.52	1.04235	100

Figures 4 and 5 illustrate the force variations depending on the velocity and the variations of the normalized velocity as a function of the normalized force. In addition, the "trendline" regression curves in the form of power are presented, which are close to the function Cv^{α} introduced by the exponent α.

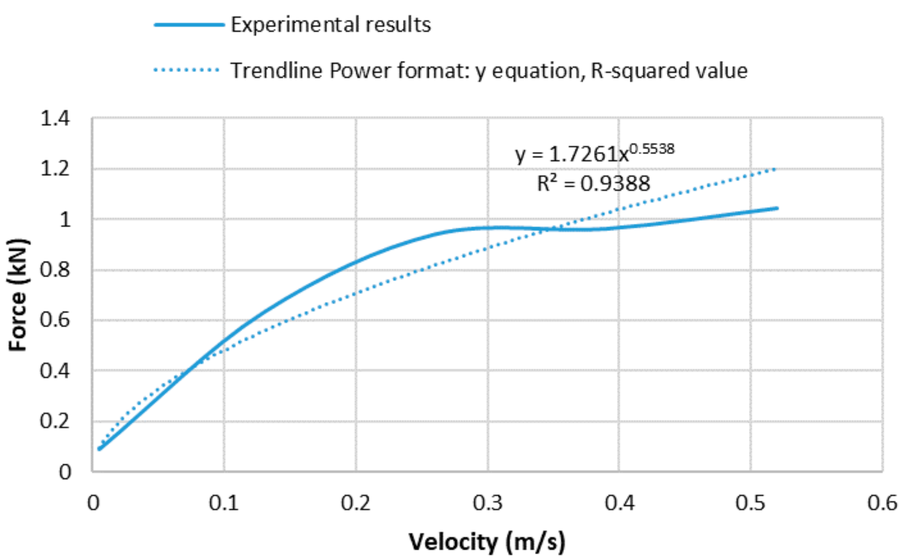

Figure 4. Force vs. velocity.

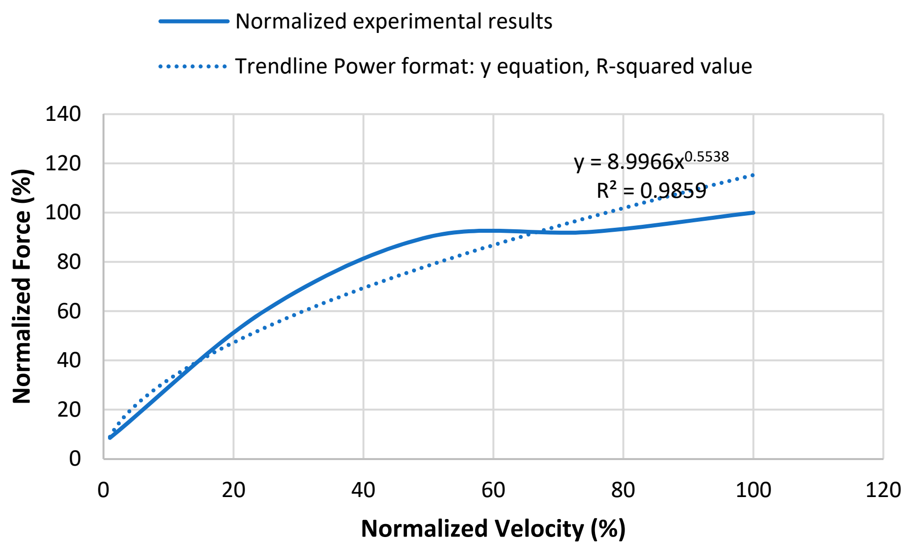

Figure 5. Normalized force vs. normalized velocity.

A typical constitutive law of an FSD, from the standard EN 15129 [1], has the equation:

$$F = F_0 + Kx + Cv^{\alpha}, \tag{4}$$

where:

- F_0 is the preload force (kN);
- K is the stiffness (kN/m);
- C is the damping coefficient $(\mathrm{kN}/(\mathrm{m/s})^{\alpha})$;
- α is the exponent of the constitutive law.

Even if the preload force is zero, in this case, the closest model for FSDs is the Kelvin –Voigt model (spring and damper in parallel), where the elastic stiffness describes the effect of the fluid compressibility [1].

4. An Approach of the Extended Kelvin–Voigt Model for FVD and Discussions

Using Equation (2) for the generalized Kelvin–Voigt model yields:

$$Kx^{\beta} + C\dot{x}^{\alpha} - F_{KV,g} = 0. \tag{5}$$

Considering the real values of velocity vs. reaction force from Table 2 and the extended Kelvin–Voigt model from Equation (2), a system of nonlinear equations can be written in the form:

$$\begin{cases} K\left(\frac{d_{bd}}{2}\right)^{\beta} + C(v(1))^{\alpha} - F_n(1) = 0, \\ K\left(\frac{d_{bd}}{2}\right)^{\beta} + C(v(2))^{\alpha} - F_n(2) = 0, \\ K\left(\frac{d_{bd}}{2}\right)^{\beta} + C(v(3))^{\alpha} - F_n(3) = 0, \\ K\left(\frac{d_{bd}}{2}\right)^{\beta} + C(v(4))^{\alpha} - F_n(4) = 0, \\ K\left(\frac{d_{bd}}{2}\right)^{\beta} + Cv(5)^{\alpha} - F_n(5) = 0. \end{cases} \tag{6}$$

In the previous nonlinear system (6), $v(i)$ with index $i = \overline{1\ldots5}$ are the values from the velocity column in Table 2, where it is considered that $v = \dot{x}$. Using the extended Kelvin–Voigt model, the values of the restoring force, F_n, must satisfy this relation, and, therefore, at 50% of $-d_{bd}$ and $+d_{bd}$ can be considered as $2F_n = F_{KV,g}^{(+)} + \left|F_{KV,g}^{(-)}\right|$ or $F_n = F_{KV,g}$. In the supposed system, the values of the force $F_n(i)$ with index $i = \overline{1\ldots5}$ are the values from the reaction force column in Table 2.

Using the experimental values presented in Table 2, the nonlinear differential system (6) yields the unknown parameters of the system (6) K, C, α, and β.

Using the MATLAB Software to solve the nonlinear system (6), we determined the unknown parameters K, C, α, β and the variation of the force vs. the velocity. Figure 6 illustrates the differences between the experimental tests and the implementation of the extended Kelvin–Voigt model.

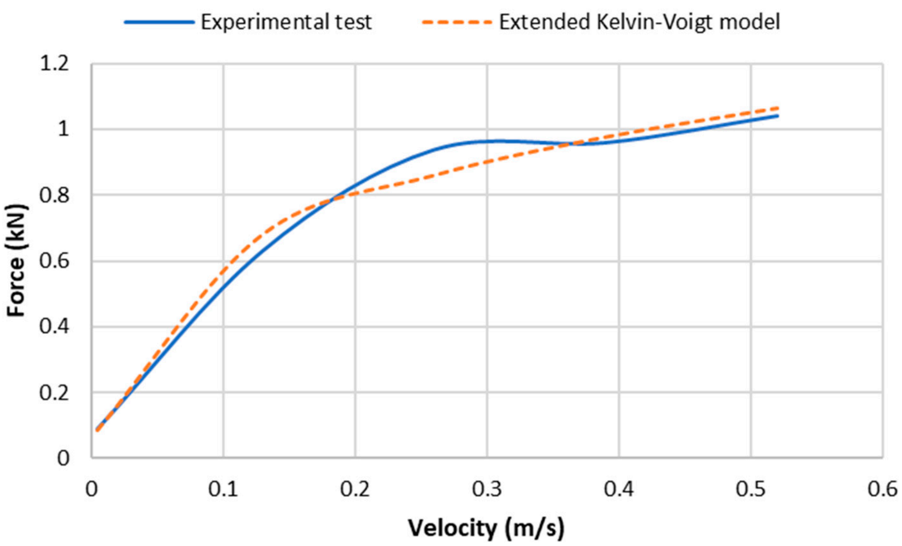

Figure 6. Force vs. velocity: Experimental tests and extended Kelvin–Voigt model.

As seen from Figure 6, the standard deviation has a maximum value of 5.6% at a velocity of 0.26 m/s between the experimental tests and the extended Kelvin–Voigt model for which the constitutive law parameters were computed using the nonlinear differential system (6). Table 3 lists the values of the correlations between the experimental data and the extended Kelvin–Voigt model.

Table 3. The correlation between the experimental values and the extended Kelvin–Voigt model.

No./ Index	Velocity v [m/s]	Experimental Data of the Restoring Force F_n [kN]	Generalized Kelvin-Voigt Model-Restoring Force F_n [kN]	Standard Deviation [%]
1	0.0052	0.08889	0.0865	0.17
2	0.13	0.63013	0.6800	3.53
3	0.26	0.93926	0.8601	5.60
4	0.39	0.96099	0.9765	1.10
5	0.52	1.04235	1.0640	1.53

It can be concluded, by analyzing the data presented in Table 3 and Figure 6, that the proposed approach for the velocity-dependent fluid viscous damper, the extended Kelvin–Voigt model, agrees with the experimental data of the nonlinear viscous damper in the entire range of the velocity.

5. Conclusions

This work presents a method of implementing the extended Kelvin–Voigt rheological model to identify the constitutive law's parameters for the dynamic behavior of FVDs. The experimental results performed on an FVD to determine the parameters of the law of conduct validated the results obtained with the extended Kelvin–Voigt method based on the variation of the restoring force, F_n, depending on the velocity steps, v. Based on the five sets of values required by the standard EN 15129 [1] at 1%, 25%, 50%, 75%, and 100% of the maximum velocity, a nonlinear set of five equations can be formed that meet the conditions of the extended Kelvin–Voigt model (see Equation (6)). Comparing the values illustrated in Figure 6 and Table 3, it can be concluded that the extended Kelvin–Voigt model is close to the experimental results.

This practical approach can aid specialists in seismic devices to identify the law of behavior for FVDs or FSDs and its parameters after performing the experimental tests that are imposed by EN 15129 [1].

Author Contributions: Conceptualization, O.V. and M.B.; methodology, O.V. and M.B.; software, O.V.; validation, O.V. and M.B.; formal analysis, O.V.; investigation, O.V. and M.B.; resources, O.V.; data curation, O.V.; writing—original draft preparation, O.V. and M.B.; writing—review and editing, M.B.; visualization, O.V. and M.B.; supervision, O.V. and M.B.; project administration, O.V. and M.B. All authors have read and agreed to the published version of the manuscript.

Funding: This research received no external funding.

Data Availability Statement: Not applicable.

Acknowledgments: The authors of this article are thankful to the University POLITEHNICA of Bucharest for providing a serene environment and the facilities to carry out this research work.

Conflicts of Interest: The authors declare no potential conflict of interest concerning this article's research, authorship, and/or publication.

References

1. European Standard EN 15129, 2009—Anti-Seismic Devices. Available online: https://www.en-standard.eu/csn-en-15129-anti-seismic-devices/ (accessed on 20 November 2022).
2. Sadek, F.; Riley, M. Design Procedures for Structures with Supplemental Dampers, Wind and Seismic Effects. In Proceedings of the 32nd Joint Meeting of the U.S.-Japan Cooperative Program in Natural Resources; Panel on Wind and Seismic Effects, Tokyo, Japan, 16–19 May 2000. Available online: https://www.nist.gov/publications/design-procedures-structures-supplemental-dampers (accessed on 20 November 2022).
3. Verma, N.P. Viscous Dampers for Optimal Reduction in Seismic Response. Master of Science Thesis, MS in Engineering Mechanics granted by University Virginia Tech, Blacksburg, VA, USA, 11 July 2001. Available online: https://vtechworks.lib.vt.edu/handle/10919/43716 (accessed on 20 November 2022).
4. Berkovsky, A.; Vasilyev, P.; Kireev, O. Different Approaches for the Modelling of High Viscous Dampers in Piping Dynamic Analysis. Acceptable Limits for Simplifications. In Proceedings of the 20 International Conference on Structural Mechanics in Reactor Technology SMIRT 20, Espoo, Finland, 9–14 August 2009; Paper 1833. Available online: https://www.semanticscholar.org/paper/Different-Approaches-for-the-Modelling-of-High-in-Berkovskya-Vasilyeva/e7b0b8274f9ce7f2c1ff62a99e85f858f4aaed6d (accessed on 20 November 2022).
5. Whittle, J.; Williams, M.S.; Blakeborough, A. Preliminary Study of Optimal Placement of Viscous Dampers in Buildings. In Proceedings of the 10th Canadian Conference on Earthquake Engineering, Toronto, ON, Canada, 25–29 July 2010; Paper 361. pp. 6346–6355. Available online: https://ora.ox.ac.uk/objects/uuid:6641c63e-d156-4cbb-a550-b052ae16bd75 (accessed on 20 November 2022).
6. Seleemah, A.A.; Constantinou, M.C. *Investigation of Seismic Response of Buildings with Linear and Nonlinear Fluid Viscous Dampers*; Technical Report NCEER-97-0004; State University of New York: Buffalo, NY, USA, 1997. Available online: https://www.researchgate.net/publication/274373766_Investigation_of_Seismic_Response_of_Buildings_with_Linear_and_Nonlinear_Fluid_Viscous_Dampers (accessed on 12 December 2022).
7. Martinez-Rodrigo, M.; Romero, M.L. An optimum retrofit strategy for moment resisting frames with nonlinear viscous dampers for seismic applications. *Eng. Struct.* **2003**, *25*, 913–925. [CrossRef]
8. Greco, R.; Marano, G.C. Identification of parameters of Maxwell and Kelvin–Voigt generalized models for fluid viscous dampers. *J. Vib. Control.* **2015**, *21*, 260–274. [CrossRef]
9. Xu, J.H.; Li, A.Q.; Shen, Y. Fractional-Derivative Maxwell Kelvin Model for "5+4" Viscoelastic Damping Wall subjected to Large Deformation. *Math. Probl. Eng.* **2016**, *2016*, 3170967. [CrossRef]
10. Park, S.W. Analytical modeling of viscoelastic dampers for structural and vibration control. *Int. J. Solids Struct.* **2001**, *38*, 8065–8092. [CrossRef]
11. Lewandowski, B.; Chorazyczewski, B. Identification of the parameters of the Kelvin-Voigt and Maxwell fractional models, used to modeling of viscoelastic dampers. *Comput. Struct.* **2010**, *88*, 1–17. [CrossRef]

12. Castellano, M.G.; Borelia, R.; Infanti, S. Experimental Characterization of Nonlinear Fluid Viscous Dampers according to the New European Standard. In Proceedings of the 5th European Conference on Structural Control EACS 2012, Genoa, Italy, 18–20 June 2012; Paper No. 143. Available online: https://www.academia.edu/29366170/Experimental_characterization_of_nonlinear_fluid_viscous_dampers_according_to_the_New_European_Standard (accessed on 20 November 2022).
13. Mousavi, D.A.; Ghorbani-Tanha, S.A. Optimum placement and characteristics of velocity-dependent dampers under seismic excitation. *Earthq. Eng. Eng. Vib.* **2012**, *11*, 403–414. [CrossRef]
14. Pettinga, J.D.; Oliver, S.; Kelly, T.E. A design office approach to supplemental damping using fluid viscous dampers. In Proceedings of the Steel Innovations Conference, Christchurch, New Zealand, 21–22 February 2013. Available online: https://www.semanticscholar.org/paper/A-DESIGN-OFFICE-APPROACH-TO-SUPPLEMENTAL-DAMPING-Oliver/825ccfc0a9cd01a5396e4239f421df1653f6b81f (accessed on 20 November 2022).
15. Cavaleri, L.; Di Trapani, F.; Ferrotto, M.F. Experimental determination of viscous damper parameters in low velocity ranges. *Int. J. Earthq. Eng. Ing. Sismica* **2017**, *34*, 64–74.
16. Del Gobbo, G.M. Placement of Fluid Viscous Dampers to Reduce Total-Building Seismic Damage. Ph.D. Thesis, Granted by University of Oxford, Oxford, UK, 2017. Available online: https://ora.ox.ac.uk/objects/uuid:29da2030-ff4e-4435-ad29-5855e503e05 (accessed on 20 November 2022).
17. Lampres-Pineda, A.C.; Garzon-Amortegui, L.F. Nonlinear Viscous Fluid Damping Devices in the Seismic Design of Buildings. Master's Thesis, Granted by Politecnico di Milano, Milano, Italy, 2018. Available online: https://scholar.google.ro/scholar?q=NONLINEAR+VISCOUS+FLUID+DAMPING+DEVICES+IN+THE+SEISMIC+DESIGN+OF+BUILDINGS&hl=en&as_sdt=0&as_vis=1&oi=scholart (accessed on 20 November 2022).
18. Wong, K.K.F. Seismic energy analysis of structures with nonlinear fluid viscous dampers-algorithm and numerical verification. *Struct. Des. Tall Spec. Build.* **2011**, *20*, 482–496. [CrossRef]
19. Altieri, D.; Tubaldi, E.; De Angelis, M.; Patelli, E.; Dall'Asta, A. Reliability-based optimal design of nonlinear viscous dampers for the seismic protection of structural systems. *Bull. Earthq. Eng.* **2018**, *16*, 963–982. [CrossRef]
20. Bougteb, Y.; Ray, T. Choice between series and parallel connections of hysteretic system and viscous damper for seismic protection of structures. *Eng. Struct. Dyn.* **2017**, *47*, 237–244. [CrossRef]
21. Noruzvand, M.; Mohebbi, M.; Shakeri, K. Modified direct displacement-based design approach for structures equipped with fluid viscous damper. *Struct. Control. Health Monit.* **2020**, *27*, 19. [CrossRef]
22. De Domenico, D.; Hajirasouliha, I. Multi-level performance-based design optimization of steel frames with nonlinear viscous dampers. *Bull. Earthq. Eng.* **2021**, *19*, 5015–5049. [CrossRef]
23. Michailides, C. VD-PQ; A Velocity-Dependent Viscous Damping Model for Wave-Structure Interaction Analysis. *J. Mar. Sci. Eng.* **2021**, *9*, 175. [CrossRef]
24. Kookalani, S.; Shen, D. Effect of Fluid Viscous Damper parameters on the seismic performance. *J. Civil. Eng. Mater. App.* **2020**, *4*, 141–153. [CrossRef]
25. Vaiana, N.; Napolitano, C.; Rosati, L. Some recent advances on the modeling of the hysteretic behavior of rate-independent passive energy dissipation devices. In Proceedings of the Proceedia ECCOMAS of 8th ECCOMAS Conference on Computational Methods in Structural Dynamics, Athens, Greece, 28–30 June 2021. [CrossRef]
26. Symans, M.D.; Charney, F.A.; Whittaker, A.S.; Constantinou, M.C.; Kircher, C.A.; Johnson, M.W.; McNamara, R.J. Energy dissipation systems for seismic applications: Current practice and recent developments. *J. Struct. Eng.* **2008**, *134*, 3–21. [CrossRef]
27. Constantinou, M.C.; Symans, M.D. Seismic response of structures with supplemental damping. *Struct. Des. Tall Spec. Build.* **1993**, *2*, 77–162. [CrossRef]
28. Vaiana, N.; Rosati, L. Classification and unified phenomenological modeling of complex uniaxial rate-independent hysteretic responses. *Mech. Syst. Signal Proc.* **2022**, *192*, 109539. [CrossRef]
29. Vaiana, N.; Capuano, R.; Rosati, L. Evaluation of path-dependent work and internal energy change for hysteretic mechanical systems. *Mech. Syst. Signal Proc.* **2022**, *186*, 109962. [CrossRef]